Research and Reviews in Materials Science and Chemistry
Vol. 7, Issue 1, 2016, Pages 1-24
ISSN 2319-6920
Published Online on September 19, 2016

http://jyotiacademicpress.org

SYNTHESIS, CRYSTAL STRUCTURE AND VIBRATIONAL PROPERTIES OF N-(2-AMMONIUM ETHYL)-PROPANE-1,3DIAMMONIUM HEXACHLOROBISMUTHATE(III)

MARWA BEN TAHER, NAJLA CHAARI, HIBA KHILI and SLAHEDDINE CHAABOUNI

Laboratoire des Sciences des Matériaux et d'Environnement
Faculté des Sciences de Sfax
Université de Sfax
BP 1171, Route de Soukra
3018 Sfax
Tunisia
e-mail: marwabentaher@yahoo.fr

Abstract

A new organic-inorganic crystal, N-(2-ammonium ethyl)-propane-1,3diammonium hexachlorobismuthate(III) has been synthesized by the slow evaporation method at room temperature and characterized by X-ray diffraction, thermal analyse (DSC), spectroscopic FT-IR and Raman. The single X-ray diffraction studies have revealed that the compound crystallizes in monoclinic non-centrosymmetric space group Pn, the crystal is built up of separated $BiCl_6^{3-}$ octahedral anions and N-(2-ammonium ethyl)-propane-1,3diammonium cations. The cohesion of the structure is achieved by an extensive network of N–H…Cl hydrogen bonds between the N-(2-ammonium ethyl)-propane-1,3diammonium

Keywords and phrases: organic-inorganic hybrid material, DSC, phase transition, IR absorption, Raman scattering.

Communicated by Ana Rosa Silva.

Received June 30, 2016; Revised August 27, 2016

cations and the octahedra $[BiCl_6]^{3-}$ anions, in which they may be effective in the stabilization of the crystal structure. Differential scanning calorimetry (DSC) disclosed structural phase transition of the order-disorder type at 398K. The Raman studies of the polycrystalline $[NH_3(CH_2)_3NH_2(CH_2)_2NH_3]BiCl_6$ performed in the frequency region between $3500cm^{-1}$ and $50cm^{-1}$ show that the vibrational state of N-(2-ammonium ethyl)-propane-1,3diammonium cation does not change around the phase transition point.

1. Introduction

The compounds possessing organic cations and inorganic anions are of considerable interest because of their supramolecular networks. These later become more fascinating when the relevant cation and the anion can take part in hydrogen bonding interactions. The hydrogen bond are usually recognized as the most powerful tool for generating supramolecular assemblies of molecules [1].

The alkylammonium halogenoantimonates (III) and halogenobismuthates (III) of the general formula $R_xM_yX_{x+3y}$ (where R: denotes organic cations, M: Sb^{3+} or Bi^{3+}, X : Cl^-, Br^-, I^-) evoke much interest because of their ferroelectric properties. These types of crystals form various structures, mainly with an anionic sublattice built-up of the MX_6 octahedra sharing corners, edges or faces. The anionic metal-halide species has been observed to range in dimensionality from two-dimensional or one-dimensional polymeric anions to discrete anions of various sizes. In the majority of these hybrid materials the anionic moieties are rigid. The alkylammonium cations located in the cavities formed by anionic sublattices are usually making rotational motions in high temperature phases. The ferroelectric activity in these organic-inorganic crystals is generally related to ordering processes of alkylammonium cations.

The halogenoantimonates (III) and halogenobismuthates (III) with organic cations can be obtained by reacting an organic substance and antimony (III)/bismuth (III) salt (oxide) in the appropriate solvent. A wide range of ferroelectric orders of the dipoles has generally been found in compounds containing small sized ammonium cations (like monomethyl-, dimethyl- or trimethyl-ammonium) [2], [3], [4], [5], and [6].

By extending our researches to others halogenoantimonates (III) and halogenobismuthates (III) compounds, it seems interesting to undertake an X-ray, DSC and spectroscopy studies of $[NH_3(CH_2)_3NH_2(CH_2)_2NH_3]BiCl_6$ crystal, the crystal structure has been shown to belong at room temperature to monoclinic system in Pn space group. The lattice parameters are: a (Å) = 7.763(5), b (Å) = 12.679(5), c (Å) = 8.315(5), β (°) = 91.702(5), (Z = 2). The anionic sublattice in this crystal consists of isolated octahedral $BiCl_6^{3-}$. The cations are linked to the anionic sublattice units by relatively weak N–H…Cl hydrogen bonds.

In this work, we present the result of the structural study of the $[NH_3(CH_2)_3NH_2(CH_2)_2NH_3]\,BiCl_6$ compound. To detect the possible phase transitions in $[NH_3(CH_2)_3NH_2(CH_2)_2NH_3]\,BiCl_6$, we use differential scanning calorimetry (DSC). The FT-IR and FT-Raman technics show the spectroscopic properties of different chloro-and bromobismuthates (III) salts known up to now and to discuss the dynamical states of the N-(2-ammonium ethyl)-propane-1,3diammonium cations in $[NH_3(CH_2)_3NH_2(CH_2)_2NH_3]BiCl_6$.

2. Experimental Details

2.1. Preparation of single crystal

A solution of N-(2-aminoethyl)-propane-1,3diamine in HCl was added to a solution of bismuth trichloride in a minimum volume of water and a concentrated hydrochloric acid. The resulting solution was left to evaporate at room temperature. After several days, white and parallel-epepidic monocrystals appeared in the solution.

Table 1. Crystal data, summary of intensity data collection and structure refinement

Compound	$[NH_3(CH_2)_3NH_2(CH_2)_2NH_3]\ BiCl_6$
Molecular weight	550.905
Color/shape	white/parallelepepidic
Space group	Pn
Temperature (K)	296(2)
Cell constants	
a (Å)	7.763(5)
b (Å)	12.679(5)
c (Å)	8.315(5)
$\alpha(^\circ)$	90.000(5)
$\beta(^\circ)$	91.702(5)
$\gamma(^\circ)$	90.000(5)
Cell volume (Å3)	818.1(8)
Formula units/unit cell	2
$P_{calc..}(g\ cm^{-3})$	2.684
Diffractometer/scan	APEXII CCD diffractometer
Radiation. Graphite monochromator	Mo Ka (k = 0.71069Å)
$\mu calc.(mm^{-1})$	12.239
(Rint)	0.057
Unique Reflections	4904
$\theta(^\circ)$ range	$1.61 \le \theta \le 26.51$
Reflections with I > 4r(Fo)	4047
Range of h.k.l	$-9 \le h \le 9$
	$-15 \le k \le 15$
	$-10 \le l \le 9$

Table 1. (Continued)

F(000)	620.0
Weights	$w = 1/[\sigma^2(Fo^2) + (0.0433P)^2]$, where
	$P = \text{maximum } [(Fo^2.0) + 2Fc^2]/3$
$R = \sum \|\|F_0\| - \|F_c\|\| / \sum \|F_0\|$	0.057
RW	0.12

Table 2. Atomic coordinates and Ueq or Uiso for $[NH_3(CH_2)_3NH_2(CH_2)_2NH_3]BiCl_6$

Atoms	**X**	**Y**	**Z**	$\mathbf{U_{eq}}$
Bi	0.7927(9)	0.25127(5)	0.7862(9)	0.0259(3)
Cl_1	0.8138(7)	0.3950(5)	0.5424(7)	0.0544(15)
Cl_2	1.0662(5)	0.1408(4)	0.6738(5)	0.0374(11)
Cl_3	1.0090(7)	0.3628(4)	0.9765(8)	0.0487(14)
Cl_4	0.7543(6)	0.0966(4)	1.0019(6)	0.0425(12)
Cl_5	0.5367(6)	0.3575(4)	0.9241(6)	0.0418(12)
Cl_6	0.5703(6)	0.1323(4)	0.5986(7)	0.0443(13)
C_1	1.315(3)	0.3805(14)	0.566(3)	0.038(5)
C_2	1.266(3)	0.3864(16)	0.384(4)	0.061(8)
C_3	1.347(4)	0.306(3)	0.287(4)	0.068(10)
C_4	1.344(3)	0,1115(17)	0.205(2)	0.037(4)
C_5	1.269(3)	0,1198(19)	0.047(3)	0.043(5)
N_1	1.237(3)	0,4602(15)	0.669(2)	0.051(5)
N_2	1.277(2)	0.1940(12)	0.325(2)	0.035(3)
N_3	1.342(2)	0.0365(13)	– 0.063(2)	0.043(4)

Table 2. (Continued)

H_{11}	1.1224	0.4549	0.6612	0.076
H_{12}	1.2718	0.4499	0.7705	0.076
H_{13}	1.2686	0.5242	0.6374	0.076
H_1A	1.2824	0.3114	0.6049	0.046
H_1B	1.4388	0.3864	0.5781	0.046
H_2A	1.3112	0.1756	0.4259	0.042
H_2B	1.1614	0.1949	0.3205	0.042
H_2C	1.1417	0.3797	0.3705	0.073
H_2D	1.2978	0.4552	0.3437	0.073
H_{31}	1.2951	0.0434	– 0.1610	0.064
H_{32}	1.3184	– 0.0273	– 0.0245	0.064
H_{33}	1.4558	0.0445	– 0.0667	0.064
H_3A	1.4704	0.3077	0.3078	0.081
H_3B	1.3252	0.3215	0.1741	0.081
H_4A	1.4677	0.1190	0.1986	0.045
H_4B	1.3209	0.0415	0.2466	0.045
H_5B	1.1448	0.1110	0.0518	0.051

Table 3. Anisotropic displacement parameters (Å²) for $[NH_3(CH_2)_3NH_2(CH_2)_2NH_3]BiCl_6$

Atoms	U11	U22	U33	U32	U13	U12
Bi	0.0342(5)	0.0223(5)	0.0211(5)	– 0.0004(2)	0.0020(3)	– 0.0007(2)
Cl_1	0.059(3)	0.055(3)	0.050(3)	0.026(3)	0.013(3)	0.008(3)
Cl_2	0.038(2)	0.045(3)	0.029(2)	– 0.004(2)	0.0019(18)	0.003(2)
Cl_3	0.051(3)	0.034(3)	0.060(4)	– 0.012(2)	– 0.015(3)	0.002(2)
Cl_4	0.054(3)	0.037(2)	0.037(3)	0.014(2)	– 0.001(2)	0.002(2)
Cl_5	0.049(3)	0.040(3)	0.036(3)	– 0.003(2)	0.008(2)	0.005(2)
Cl_6	0.046(3)	0.042(3)	0.045(3)	– 0.011(2)	– 0.013(2)	0.007(2)
C_1	0.067(14)	0.014(8)	0.034(11)	0.010(7)	– 0.008(10)	0.005(8)
C_2	0.060(14)	0.019(9)	0.10(2)	– 0.041(13)	– 0.017(14)	0.006(10)
C_4	0.038(10)	0.043(11)	0.031(10)	0.015(8)	0.010(8)	0.011(8)
C_5	0.044(12)	0.054(13)	0.030(11)	0.006(9)	– 0.008(9)	0.008(9)
N_1	0.061(11)	0.048(10)	0.044(10)	– 0.013(9)	0.004(9)	– 0.012(9)
N_2	0.042(8)	0.031(8)	0.032(8)	0.003(7)	0.014(7)	– 0.005(8)
N_3	0.050(9)	0.043(9)	0.036(9)	0.015(7)	0.004(8)	0.000(8)

2.2. X-Ray diffraction

The X-ray data collection was carried out on a Bruker APEXII CCD four circle diffractometer using MoKα radiation. The positional parameters for the heavy atoms were obtained from a three-dimensional Patterson map, while the non H-atoms were found from successive difference Fourier maps. The structure was refined by full-matrix least squares using anisotropic temperature factors for all non-hydrogen atoms and the hydrogen atoms were localized and optimized to restrained positions. Calculations were performed with the programs SHELXS and SHELXL [9], using the scattering factors enclosed therein. The crystal data, collected reflections and parameters of the final refinement are reported in Table 1. Interatomic distances, bond angles and hydrogen bonds schemes are listed in Tables 4 and 5.

Table 4. Principal intermolecular distances (Å) and angles (°) in $[NH_3(CH_2)_3NH_2(CH_2)_2NH_3]BiCl_6$

Bond lengths (Å) and angles (°)			
$Bi - Cl_1$	2.734(8)	$C_1 - N_1$	1.47(3)
$Bi - Cl_2$	2.731(8)	$C_1 - C_2$	1.55(4)
$Bi - Cl_3$	2.677(8)	$C_2 - C_3$	1.45(4)
$Bi - Cl_4$	2.680(7)	$N_2 - C_3$	1.56(4)
$Bi - Cl_5$	2.686(8)	$N_2 - C_4$	1.55(3)
$Bi - Cl_6$	2.743(8)	$C_5 - C_4$	1.43(3)
		$C_5 - N_3$	1.52(3)
$Cl_3 - Bi - Cl_4$	94.1(3)	$C_4 - C_5 - N_3$	110.6(2)
$Cl_3 - Bi - Cl_5$	86.7(2)	$C_4 - N_2 - C_3$	111.2(2)
$Cl_4 - Bi - Cl_5$	89.0(3)	$C_5 - C_4 - N_2$	114.2(2)
$Cl_3 - Bi - Cl_2$	89.6(3)	$N_1 - C_1 - C_2$	116.4(2)
$Cl_4 - Bi - Cl_2$	87.53(2)	$C_3 - C_2 - C_1$	114(2)
$Cl_5 - Bi - Cl_2$	174.7(3)	$C_2 - C_3 - N_2$	112(2)
$Cl_3 - Bi - Cl_1$	92.0(2)		
$Cl_4 - Bi - Cl_1$	173.7(3)		
$Cl_5 - Bi - Cl_1$	92.5(2)		
$Cl_2 - Bi - Cl_1$	91.3(3)		
$Cl_3 - Bi - Cl_6$	178.2(3)		
$Cl_4 - Bi - Cl_6$	84.1(2)		
$Cl_5 - Bi - Cl_6$	93.3(3)		
$Cl_2 - Bi - Cl_6$	90.3(2)		
$Cl_1 - Bi - Cl_6$	89.7(3)		

Table 5. Interatomic distances (Å) and bond angles (°) involved in the hydrogen bonds of $[NH_3(CH_2)_3NH_2(CH_2)_2NH_3]BiCl_6$ compound

Hydrogen bonds	D–H (Å)	H...A (Å)	D...A(°)	D–H...A (Å)	A
$N_2 - H_{2A}$	0.900	2.497	143.07	3.262(2)	Cl_6^{i}
$N_2 - H_{2A}$	0.900	2.880	121.58	3.438(1)	Cl_2
$N_3 - H_{31}$	0.890	2.535	143.86	3.296(2)	Cl_2^{ii}
$N_3 - H_{32}$	0.890	2.578	140.82	3.316(2)	Cl_6^{iii}
$N_3 - H_{32}$	0.890	2.881	121.09	3.426(2)	Cl_2^{iii}
$N_3 - H_{33}$	0.890	2.460	161.85	3.317(2)	Cl_4^{iv}
$N_1 - H_{12}$	0.890	2.659	137.01	3.366(2)	Cl_5^{v}
$N_1 - H_{12}$	0.890	2.919	114.40	3.385(2)	Cl_3
$N_1 - H_{11}$	0.890	2.674	158.11	3.516(2)	Cl_1
$N_1 - H_{13}$	0.890	2.734	145.25	3.502(2)	Cl_3^{vi}
$N_1 - H_{13}$	0.890	2.907	118.49	3.422(2)	Cl_5^{vi}

2.3. Differential scanning calorimetry

Differential scanning calorimetry (DSC) measurements were carried out on a Perkin-Elmer DSC-7 calorimeter. The differential scanning calorimetry was recorded in the 298K-500K region.

2.4. The infrared (IR) spectrum

For the infrared measurement, a small quantity of the powder was used. The infrared (IR) spectrum was recorded at room temperature in the $4000cm^{-1}$-$400cm^{-1}$ region using a KBr pellet on Perkin Elmer spectrometer.

2.5. Raman spectrum

Raman spectra were recorded with a LABRAMHR 800 triple monochromator over the wavenumber range $3500cm^{-1}$-$50cm^{-1}$.

3. Results and Discussion

3.1. X-Ray studies

The final atomic coordinates obtained from the single crystal refinement with Ueq are given in Table 2, Table 3 shows the anisotropic displacement parameters. Interatomic distances and bond angles schemes are listed in Table 4.

The first tentative of resolution of the structure shows that the title compound crystallizes at room temperature in $P2_1/n$: one bismuth and three chlorine, and the half of the organic molecule were positioned, the rest was found by symmetry, but because we can not assimilate nitrogen to carbon by symmetry this attempt was rejected (Figure 1), the structure was therefore resolved in the non-centrosymmetric space group Pn, with the following lattice parameters: a = 7.763(5)Å, b = 12.679(5)Å, $c = 8.315(5)Å, \beta = 91.702(5)^{\circ}, D_m = 2.432gcm^{-3}$, and $D_c = 2.684gcm^{-3}, Z = 2$. The structure was solved by the Patterson method and subsequent difference Fourier synthesis. It was refined in the full-matrix least squares method using anisotropic temperature factors.

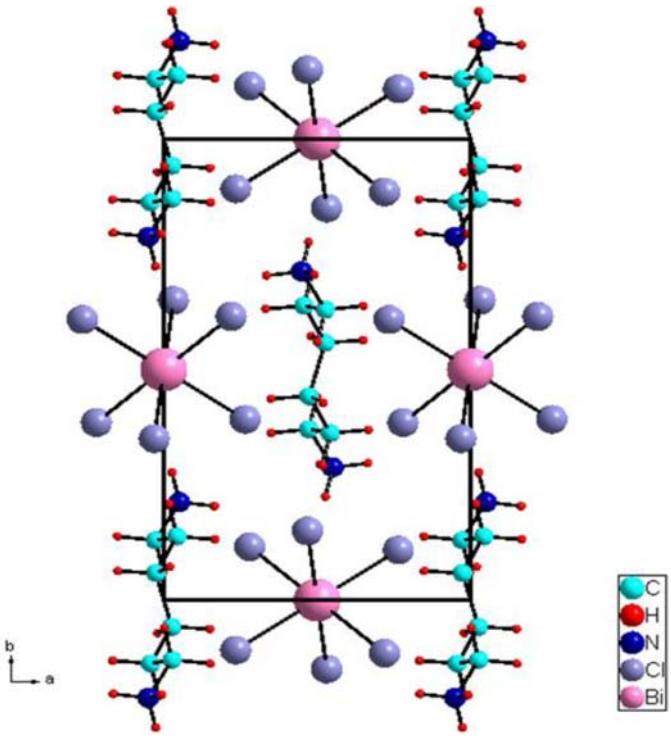

Figure 1. Projection along the c axis of the atomic arrangement of $[NH_3(CH_2)_3NH_2(CH_2)_2NH_3]BiCl_6$ in $P2_1/n$.

The crystallographic analysis of the title compound reveal that the crystal structure of $[NH_3(CH_2)_3NH_2(CH_2)_2NH_3]BiCl_6$ consists of monomeric $[BiCl_6]^{3-}$ octahedra and one crystallographically independent N-(2-ammonium ethyl)-propane-1,3diammonium.

An examination of the structure shows that the organic and inorganic groups alternate, whatever direction is chosen (Figures 1 and 2).

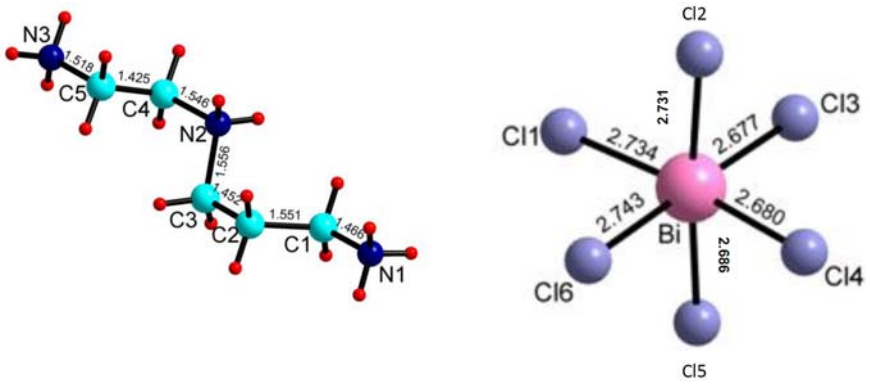

Figure 2. Atom numbering scheme for the title compound $[NH_3(CH_2)_3NH_2(CH_2)_2NH_3]BiCl_6$.

Each Bi atom is surrounded by six Cl atoms forming a weakly distorted octahedral configuration, with Bi–Cl bond lengths ranging from 2.677(8)Å to 2.743(8)Å. The cis Cl–Bi–Cl angles are between 84.1(2)° to 94.1(3)°, wheras the trans angles range from 110.6(1)° to 178.2(3)° (Figure 3).

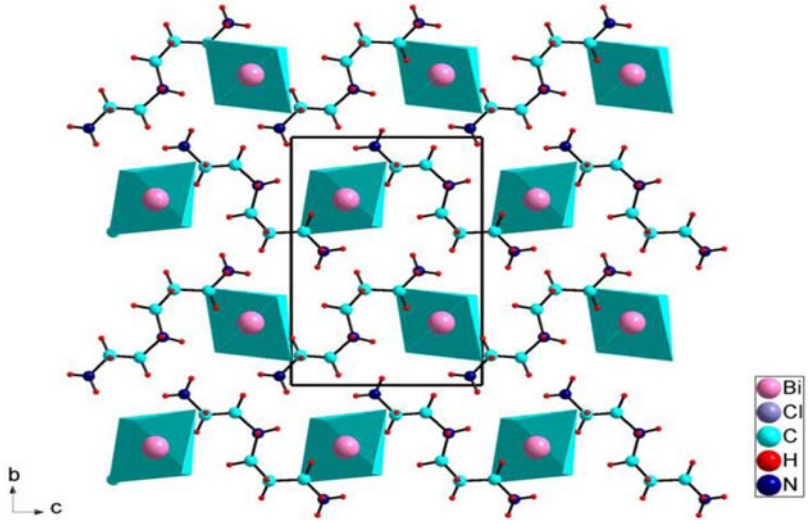

Figure 3. Projection in the (b. c) plan for the atomic arrangement of $[NH_3(CH_2)_3NH_2(CH_2)_2NH_3]BiCl_6$.

In addition to the bond length differences, the Cl–Bi–Cl bond angles (Table 2) deviate from 90°, with the biggest difference [94.1(3)°] occurring for the Cl(3)–Bi–Cl(4) angle and the lowest one [84.1(2)°] occurring for the Cl(4)–Bi–Cl(6) angle. At room temperature the $BiCl_6$ octahedra are completely ordered. The involvement of any particular chlorine atom in hydrogen bonding brings about the shift of the lone electron pair of the Bi atom in the direction of the H atom, which generally results in the shift of the respective Cl atom out of the Bi position. This leads to an increase in the Bi–Cl bond length ($Bi–Cl_2$: 2.731(8)Å, $Bi–Cl_1$: 2.734(8)Å, and $Bi–Cl_6$: 2.743(8)Å) compared to the others. The lone electron pair of the Bi atom in the direction of the faces Cl_1, Cl_2, and Cl_6 of the octahedral.

The distortion index is low and the distances (Bi–Cl) are near to each other so the lone pair is inactive, the octahedron $BiCl_6^{3-}$ is almost regular.

Figure 3 shows that the N-(2-ammonium ethyl)-propane-1, 3diammonium cations are interspersed between the anionic plans cituated at $y = 1/4$ and $y = 3/4$. The C–N and C–C bond lengths vary, respectively, from 1.47(3)Å to 1.56(4)Å and 1.43(3)Å to 1.55(4)Å. These values are comparable with those reported by other researchers [7]. The $[NH_3(CH_2)_3NH_2(CH_2)_2NH_3]BiCl_6$ is stabilized by means of the N–H…Cl hydrogen bonds, forming a three-dimensional network (Table 5) such that all the hydrogen atoms bonded to nitrogen atoms participate in the formation of these hydrogen bonds, with distances between 3.262Å and 3.516Å. These connections can be classified as the rather weak hydrogen bonds [8]. Each cation forms two or three hydrogen bonds with different anions and stabilizes the cationic framework in the crystal lattice.

3.2. Differential scanning calorimetry measurements

A typical result of the calorimetric study of this compound is presented in Figure 4. DSC showed one endothermic peak detected at 398K. The shape of the observed scanning anomalie suggests the existence of one phase transition, this is confirmed by Raman measurements at different temperatures. The phase transition order was determined from the shape of the thermal anomalies, which clearly indicate the first order nature of the observed phase transition in $[NH_3(CH_2)_3NH_2(CH_2)_2NH_3]BiCl_6$.

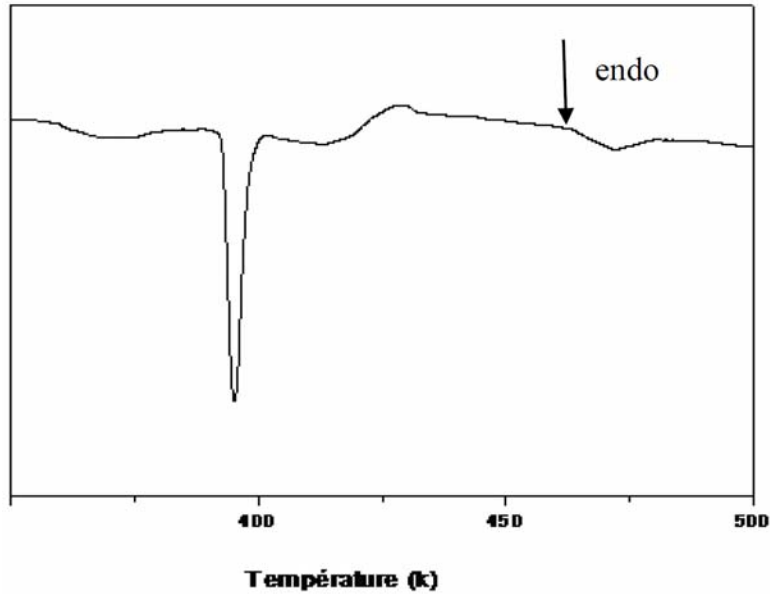

Figure 4. Differential scanning calorimetry curve of $[NH_3(CH_2)_3NH_2(CH_2)_2NH_3]BiCl_6$.

3.3. Vibrational studies

To gain more informations on the crystal structure, we have undertaken a vibrational study using infrared spectroscopy and Raman scattering. The tentative assignments of the vibrations are based on a comparison of the infrared and Raman spectra of $[NH_3(CH_2)_3NH_2(CH_2)_2NH_3]BiCl_6$ with other spectra known from the literature about numerous chlorobismuthate (III) compounds [9, 12].

The Raman and infrared peaks frequencies are quoted in Table 6.

The IR spectra of $[NH_3(CH_2)_3NH_2(CH_2)_2NH_3]BiCl_6$ (Figure 5) were recorded in the wavenumber region between $4000cm^{-1}$ and $500cm^{-1}$. The IR spectra shows at high wavenumbers, one absorption band detected at $3439cm^{-1}$, assignable to ν(N–H). The band observed at $3018cm^{-1}$ is due to ν(C–H), $\nu_s(CH_2)$, and $\nu_{as}(CH_2)$ stretching

modes. The absorption band at $2361cm^{-1}$ is associated to the ν(C–H) stretching modes. The asymmetric bending vibration of (NH) appears in two bands at $1649cm^{-1}$ and $1561cm^{-1}$. The absorption bands in the $1469cm^{-1}$-$1417cm^{-1}$ range are due to $\delta(CH_2)$. The absorption band in the $1384cm^{-1}$ is caused by δ(CNH), δ(CCH), and δ(NCH). The band at $1336cm^{-1}$ is assigned to the $\Omega(CH_2)$ and $\tau(CH_2)$. The bands at $1247cm^{-1}$, $1188cm^{-1}$, $1166cm^{-1}$, and $1096cm^{-1}$ are assigned to the δ(CH) stretching vibrations. The band observed at $1284cm^{-1}$ is due to ν_a(C–N) and $\omega(CH_2)$ stretching modes. The band at $1122cm^{-1}$ may be assigned to the deformation δ(N–H). The asymmetric bending vibration of ν_{as}(C–N) appears in two bands at $1067cm^{-1}$ and $993cm^{-1}$. The band at $923cm^{-1}$ is assigned to the rocking $r(CH_3)$ and the symmetric bending vibration of $\nu_s(CH_3)$. The absorption band at $879cm^{-1}$ is associated with ν_s(C–N) and rocking (CH_2) stretching modes. The deformations δ(CH) and rocking (CH_2) are detected at $853cm^{-1}$. The bands assigned to the $\rho(NH_3)$, $r(CH_3)$, $\rho(CH_2)$ mode are observed at $879cm^{-1}$–$750cm^{-1}$.

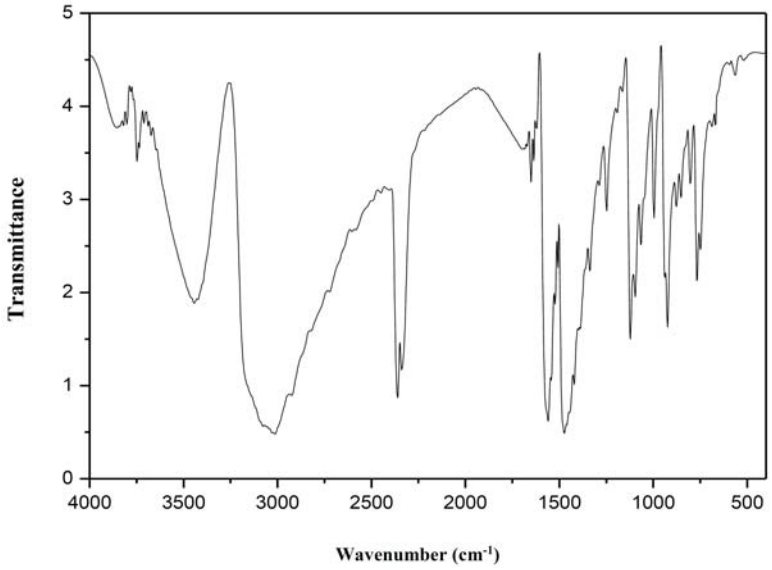

Figure 5. Infrared absorption spectrum of $[NH_3(CH_2)_3NH_2(CH_2)_2NH_3]BiCl_6$.

In the present investigation, a Raman spectroscopic measurement of N-(2-ammonium ethyl)-propane-1,3diammonium hexachlorobismuthate (III) was formed and analyzed in order to confirm the disorder degree in the different phases and the mechanism involved in the I → II transition. The Raman spectrum of $[NH_3(CH_2)_3NH_2(CH_2)_2NH_3]BiCl_6$ was recorded in the external vibrations $3500cm^{-1}$-$500cm^{-1}$. The Raman spectra at 298K, 405K, and 431K in this wavenumber region are reproduced in Figure 6. The Raman and infrared peaks frequencies are quoted in Table 6.

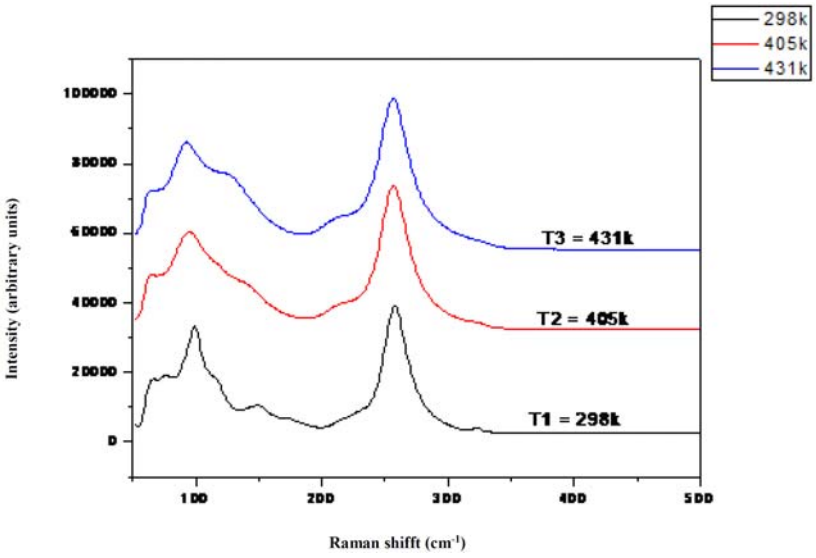

Figure 6. (a) Raman spectra of $[NH_3(CH_2)_3NH_2(CH_2)_2NH_3]BiCl_6$ in the range $50cm^{-1}$-$500cm^{-1}$ at 298K, 405K, and 431K.

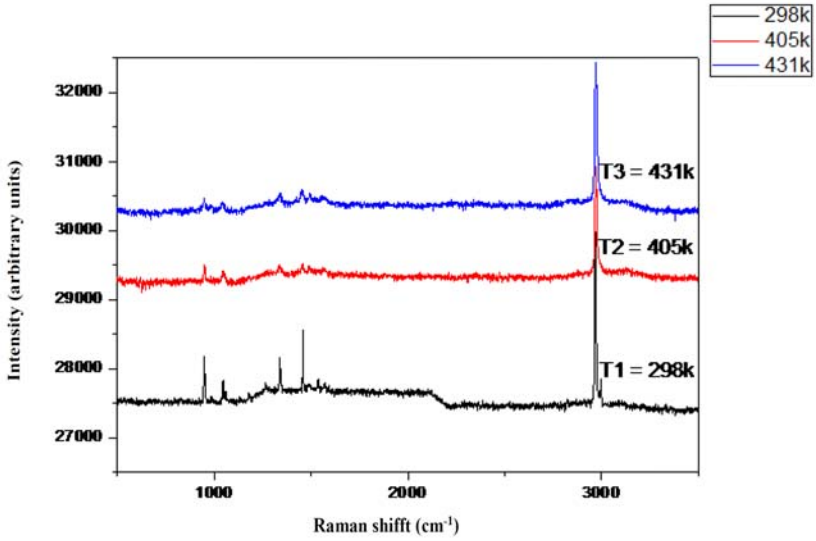

Figure 6. (b) Raman spectra of $[NH_3(CH_2)_3NH_2(CH_2)_2NH_3]BiCl_6$ in the range $500cm^{-1}$-$3500cm^{-1}$ at 298K, 405K, and 431K.

Table 6. Wavenumbers (cm^{-1}) of the bands observed in the IR and Raman spectra at 298K, 405K, and 431K of $[NH_3(CH_2)_3NH_2(CH_2)_2NH_3]BiCl_6$ and their tentative assignments (ν : stretching; δ : deformation)

FT-IR (cm^{-1})	**Raman** (cm^{-1})			**Assignments**
	298K	**405K**	**431K**	
	64.30	63.05	63.05	Lattice modes
	75.53			
	99.24	94.25	91.75	δ(Cl–Bi–Cl)
	131.68			δ_s(Cl–Bi–Cl)
	150.40			δ_s(Cl–Bi–Cl)
	257.72	257.72	256.47	νs(Bi–Cl)
	322.61			νs(Bi–Cl)
	951.15	951.15	942.38	ρ(NH_3), r(NH_3), ρ(CH_2), $\delta_s(NH_3^+)$
	1042.66	1042.66	1042.66	δ(C – H), ω(CH_2), ν_a(C–N)
	1342.15	1342.15	1333.83	δ(CNH), δ(CCH), δ(NCH), ω(CH_2)
3493.11				ν(N–H) secondary
3018.45				ν(C–H), $\nu_s(CH_2)$, $\nu_a(CH_2)$
2361.62				ν(C–H)
1649.76				δ(NH), $\delta_{as}(NH_3)$
1561.29				δ(N–H)
1469.12				δ(CH_2), $\delta_s(NH_3^+)$
1417.51	1458.61	1458.61	1450.29	δ(CNH), δ(CCH), δ(NCH)
1384.33	1342.15	1342.15	1333.83	Ω(CH_2), τ(CH_2)
1336.40				

Table 6. (Continued)

1247.92 1188.94 1166.82	1042.66	1042.66	1042.66	$\delta(CH),\ \nu_a(C-N),\omega(CH_2)$
1096.77				
1122.58				$\delta(N-H)$
1067.28				
993				$\nu_a(C-N)$
923				$r(NH_3)$
879 853 801 764	951.15	951.15	942.38	$\rho(NH_3),\ r(NH_3),\ \rho(CH_2).$ $\delta_s(NH_3^+)$
750				

The band observed at $99cm^{-1}$ was assigned to the deformation mode of Cl–Bi–Cl. The bands observed $131cm^{-1}$ and $150cm^{-1}$ arises from the symmetric deformation Cl–Bi–Cl vibration. The sharp strong shoulder at $257cm^{-1}$ and the very broad one at $322cm^{-1}$ were assigned to the Bi–Cl symmetric stretching vibration. The lattice modes can be observed in the Raman spectra between $64cm^{-1}$ and $75cm^{-1}$.

The Raman spectrum shows absorptions at $951cm^{-1}$ assignable to $\rho(NH_3)$, $r(NH_3)$, $\rho(CH_2)$, $\delta_s(NH_3^+)$ bending modes. The deformations δ(C–H), ν_a(C–N), and $\omega(CH_2)$ are detected at $1042cm^{-1}$. The band detected at $1417cm^{-1}$ is assigned to $\delta(CH_2)$, $\delta_s(NH_3^+)$ symmetric vibration while the bands observed at $1384cm^{-1}$ are attributed to (CNH), (CCH), and (NCH) bending. The symmetric bending vibration of (CH), $\omega(CH_2)$ and the deformation δ(CH) appears at $1042cm^{-1}$. The band ascribed to $\rho(NH_3)$, $r(NH_3)$, $\rho(CH_2)$, $\delta_s(NH_3^+)$ is detected at $951cm^{-1}$ (Table 7).

Table 7. Assignment of the Raman wavenumbers in the range 50-500cm^{-1} at 298K, 405K, and 431K for $[NH_3(CH_2)_3NH_2(CH_2)_2NH_3]BiCl_6$ (υ: stretching; δ : déformation)

T = 298K (Phase I)	T = 405K (Phase II)	T = 431K (Phase II)	Tentative assignment
64.30			Lattice modes
75.53	63.05	63.05	
99.24	94.25	91.75	δ(Cl–Bi–Cl)
131.68			δ_s(Cl–Bi–Cl)
150.40			δ_s(Cl–Bi–Cl)
257.72	257.72	256.47	ν_s(Bi–Cl)
322.61			ν_s(Bi–Cl)

As can be seen from Figure 6, $[NH_3(CH_2)_3NH_2(CH_2)_2NH_3]BiCl_6$ undergoes one phase transition (on heating), so on increasing the temperature of the sample from phase I to phase II, the spectral changes concern all the vibration modes of $[BiCl_6^{3-}]$. The one phase transition shown at 405K can be evidenced with the spectral transformations observed.

To increase from room temperature to 405K at low-frequency (phase I), caused the disappearance of the shoulders corresponding to the symmetric deformation mode of Cl–Bi–Cl at 130cm^{-1} and 150cm^{-1}, as well as the band at 322cm^{-1}. At the same time, there are significant changes in the positions and intensities of some bands corresponding to the internal vibrations of $[BiCl_6]^{3-}$ octahedral anions; so the bands at 130cm^{-1} and 153cm^{-1}, relative to the Cl–Bi–Cl symmetric deformation mode. The peak at 99.24cm^{-1} decreases in intensity and increases in width at half height. The two peaks at 64.30cm^{-1} and 75.53cm^{-1} coalescent in a single peak at 63cm^{-1}.

$[NH_3(CH_2)_3NH_2(CH_2)_2NH_3]BiCl_6$ undergoes one phase transition at 405K, this transition result is due to the weak perturbation of the vibrational modes of the N-(2-ammonium ethyl)-propane-1,3diammonium cations. We can observe the decrease of the bands due to $\rho(NH_3)$, $r(NH_3)$, $\rho(CH_2)$ at $951cm^{-1}$. We can see also the decrease of the band due to $\delta(CNH)$, $\delta(CCH)$, $\delta(NCH)$, and $\omega(CH_2)$ at $1342cm^{-1}$ and $\delta_{as}(NH_3^+)$, $\delta(CH_2)$ at $1458cm^{-1}$.

Shifts of the $\nu(NH^+)$, $\nu(NH_2^+)$, $\delta(NH_2^+)$, and $\delta(NH_3^+)$ vibrations, which are probably due to the formation of N–H...Cl hydrogen bonds and result from the greater rigidity of the N-(2-ammonium ethyl)-propane-1,3diammonium cations are realized. A differentiation of the cation in the unit cell appears, suggesting that the N–H...Cl hydrogen bonds are weakened [1, 12, 13-19]. This is evidence that the dynamics of the cation play a key role in the 405K phase transition indicating that the strength of the hydrogen bonds, which stabilizes the crystals, is almost independent of the anionic sublattice.

We can deduce that the changes observed in the Raman spectra are important; all the described observations indicate a possible change in the dynamical state of the transition from low to high-temperature of the $[NH_3(CH_2)_3NH_2(CH_2)_2NH_3]BiCl_6$ crystals. Furthermore, the phase transition influences the vibration of the $BiCl_6^{3-}$ anionic sublattice. This may possibly be connected to changes in the hydrogen bonding scheme above and below the phase transition points. We can conclude that the I → II transition display the order-disorder mechanism involving mainly a reorientational motion of the organic cations coupled with a distortion of the $BiCl_6$ octahedral anions.

4. Conclusion

The crystal structure of $[NH_3(CH_2)_3NH_2(CH_2)_2NH_3]BiCl_6$ was determined at room temperature; this structure (Pn, Z = 2) shows that N-(2-ammonium ethyl)-propane-1,3diammonium cations are interspersed between the anionic plans. The distortion of $BiCl_6^{3-}$ was studied by examining Bi–Cl bond lengths and Bi–Cl–Bi angles.

Most infrared and Raman bands corresponding to vibrational modes were assigned by comparison with similar compounds. Differential scanning calorimetry studies was carried out and showed the appearance of one phase transition, which was of the order-disorder type. It can be explained by the order-disorder mechanism involving mainly a reorientational motion of the organic cations coupled with distorsion of the $BiCl_6$ octahedral anions.

Acknowledgements

The crystal data collection of the title compound was done in the "Department of Chemistry, Faculty of Sciences of Sfax, University of Sfax, BP 1171, 3038 Sfax, Tunisia". We are grateful to Pr. Abdelhamid Ben Salah who supervised this experiment.

The Raman spectrum was done in "Laboratory of ferroelectric materials, Faculty of Sciences of Sfax, University of Sfax, BP 1171, 3038 Sfax, Tunisia. We are grateful to Pr. Hamadi Khemekhem for their proof reading services.

References

[1] G. Bator, R. Provoost, R. E. Silverans and Th. Zeegers-Huysken, J. Mol. Struct. 435(1) (1997), 1.

[2] G. Xu, Y. Li, W. Zhou, G. Wang, L. Cai, M. Wang, G. Guo, J. Huang, G. Bator and R. Jakubas, J. Mater. Chem. 19(15) (2009), 2179.

[3] R. Jakubas, U. Krzewska, G. Bator and L. Sobczyk, Ferroelectrics 77(1) (1988), 129.

[4] R. Jakubas, Solid State Commun. 60(4) (1986), 389.

[5] J. Zaleski, Cz. Pawlaczyk, R. Jakubas and H.-G. Unruh, J. Phys. Condens. Matter 12(33) (2000), 7509-7521.

[6] A. Miniewicz, J. Sworakowski, R. Jakubas, M. Bertault and C. Ecolivet, Ferroelectrics 94(1) (1989), 323.

[7] S. Chaabouni, S. Kamoun and J. Jaud, J. Chem. Crystallogr. 28 (1989), 209-212.

[8] G. C. Pimental and A. L. McClellan, The Hydrogen Bond, Freeman, San Fransisco, 1971.

[9] G. M. Sheldrick, Acta Crystallogr. Sect. A 64 (2008), 112-122.

[10] X. Wang and F. Liebau, Acta Crystallogr. Sect. B 52 (1996), 1-6.

[11] J. Zaleski and A. Pietraszko, Acta Crystallogr. Sect. B 52 (1996), 287-295.

[12] B. Kulicka, R. Jakubas, A. Pietraszko, G. Bator and J. Baran, Solid State Sci. 6(11) (2004), 1273.

[13] B. Bednarska-Bolek, J. Zaleski, G. Bator and R. Jakubas, J. Phys. Chem. Solids 61(8) (2000), 1249.

[14] J. Laane and P. W. Jagodzinski, Inorg. Chem. 19(1) (1980), 44.

[15] J. Tarasiewicz, R. Jakubas, J. Zaleski and J. Baran, J. Mol. Struct. 876(1-3) (2008), 86.

[16] D. Havlicek, V. Chudoba, I. Nemec, I. Cisarova and Z. Micka, J. Mol. Struct. 606(1-3) (2002), 101.

[17] L. Harry, Spell Anal. Chem. 41(7) (1969), 902.

[18] A. Marzotto, D. A. Clemente, F. Benetollo and G. Valle, Polyhedron 20(3) (2001), 171.

[19] B. Bednarska-Bolek, Z. Ciunik, R. Jakubas, G. Bator and P. Ciapala, J. Phys. Chem. Solids 63(3) (2002), 50.

■